DAAG-53-76C-0138

PREDICTED PROPERTIES OF MOSAIC IMAGES.

⑩ Tsvi Dubitzki
Narendra Ahuja
Azriel Rosenfeld

Computer Science Center
University of Maryland
College Park, MD 20742

⑮ DAAG53-76-C-0138,
DARPA Order-3206

UNIVERSITY OF MARYLAND
COMPUTER SCIENCE CENTER
COLLEGE PARK, MARYLAND
20742

(1) LEVEL II

(9) Technical rept.

(14) CSC-TR-746
DAAG-53-76C-0138

(11) March, 1979

(6) PREDICTED PROPERTIES OF MOSAIC IMAGES.

(10) Tsvi Dubitzki
Narendra Ahuja
Azriel Rosenfeld

(12) (27)

Computer Science Center
University of Maryland
College Park, MD 20742

(15) DAAG53-76-C-0138,
DARPA Order-3206

ABSTRACT

This paper considers the computation of the expected perimeter of a component in mosaic image models and checks its applicability to real images. The expected width of a component in the occupancy and Delaunay models and in a real image is also considered.

DDC

NOV 13 1979

RECEIVED

B

403 018

1. Introduction

Based on recent work in image modeling [1]-[5] it is reason-
able to try to derive real image properties from the underlying
models assumed to generate the image. Among such properties are
expected perimeter, average edge value, and expected length of a
run.

The following statistical models generating images are analyzed
in [1]-[4]: Poisson line, occupancy, and Delaunay models. The
assumption is that one of these processes generates a good approxi-
mation to a given class of natural images. The process which best
predicts the image properties will be considered to be the process
generating the image.

2. Expected perimeter

Synthetic images are easy to divide into objects and background. Thus the perimeter of the objects in such images is well defined. For digital pictures perimeter is measured by following object borders and counting vertical or horizontal moves as 1 and diagonal moves as $\sqrt{2}$. A more accurate estimate of perimeter is the average of border length as traced in the background (white) along the neighboring black points and in the object (black) along the neighboring white points. Real images must be thresholded first before measuring perimeter length. The choice of a good threshold will not be discussed here.

2.1 Synthetic images

Experiments with synthetic images were conducted using two kinds of mosaic models: occupancy and Delaunay (the dual of occupancy). Poisson line mosaics were not considered due to the errors introduced by the thickness of the lines in the digital process of random coloring of the Poisson mosaic.

Cells in the mosaic were colored randomly black with probability p and white with probability 1-p. A regular tessellation is called a KV tessellation if each cell has K neighbors and V cells meet at each vertex. In [1] it is conjectured and experimentally confirmed that a random tessellation in which the expected number of neighbors of each cell is K and the expected number of cells meeting at a vertex is V, has the same expected number of connected components as a KV randomly colored regular tessellation provided that they have the same number of cells. Under this assumption the total expected perimeter (T.E.P) of components in a mosaic is calculated as follows:

T.E.P = expected perimeter of all components

in the regular tessellation x $\dfrac{\text{expected cell perimeter}}{\text{expected number of sides of a cell}}$

Note that each grid point in a regular tessellation represents one cell in the corresponding mosaic.

Occupancy model: Here the corresponding regular tessellation is a hexagonal grid. Let S = mosaic area, λ = intensity of points

dropped on the plane to generate the mosaic nuclei. Using the
formula above and the expressions derived in [1] we get:

$$T.E.P = p \cdot \lambda \cdot S \cdot 6(1-p) \; \frac{4}{\sqrt{\lambda}} \cdot \frac{1}{6} = 4p(1-p)S\sqrt{\lambda}$$

$\frac{4}{\sqrt{\lambda}}$ is the expected perimeter in the occupancy process and the
average number of sides of a cell is 6 [5].

λ is computed as follows:

No. of cells in the mosaic x predicted No. of connected
        components per cell = observed No. of connected
                                components in the mosaic

Thus:

$$\lambda \cdot S \cdot \frac{P.N.C.C}{S'} = O.N.C.C.$$

where S = area of mosaic having 100 cells (the same as in Table
   7 [1] in order to have the same border effect).

P.N.C.C = predicted No. of connected components for the appropriate
          p in the hexagonal grid taken from Table 7 in [1].

S' = 10x10 hexagonal grid having 100 cells.

O.N.C.C = observed No. of connected components in the generated
          mosaic.

Experimental results were obtained for four mosaics. See
Figures 1(a)-1(d) for the tessellations and Figures 2(a)-2(d) for
the corresponding colored mosaics. Final judgment must be based
on the average of these results.

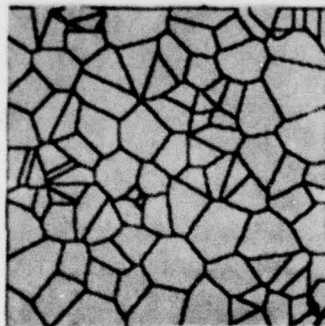The results are given in Table 1. The average deviation
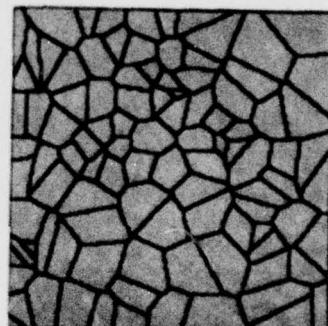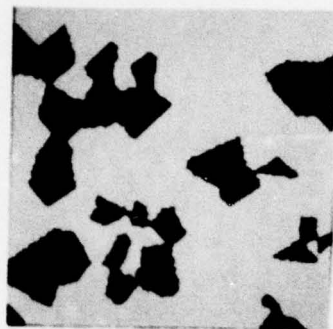between observed and predicted perimeter is very small (2.7%). The
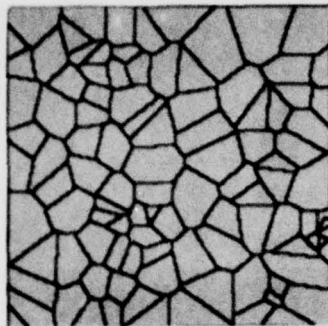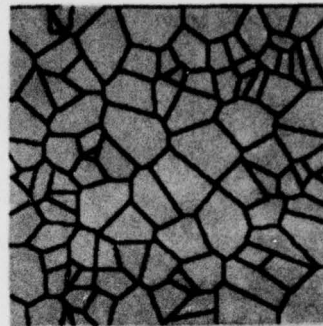
Figure 1: Occupancy tessellations ($\lambda=.003$).

(a)

(b)

(c)

(d)

Figure 2: Figures 1(a)-1(d) colored with p=.3.

Table 1: Occupancy model

Number of mosaic	Computed λ	p	O.N.C.C.	P.N.C.C.	Observed perimeter	Computed perimeter	Deviation
1	.0033	0.3	10	9.33	1570.7	1567	
2	.0036	0.3	11	9.33	1568.8	1632	
3	.0026	0.3	8	9.33	1480.7	1398	
4	.0033	0.3	11	9.33	1481.3	1632	
Average	.0033	0.3	10	9.33	1525.5	1567.6	+2.7%

Table 2: Delaunay model

| Number of mosaic	λ_0	p	O.N.C.C.	P.N.C.C.	Observed perimeter	Computed perimeter	Deviation
1	.00119	0.3	16	17.33	1771	1968	
2	.00093	0.3	13	17.33	1373	1745	
3	.00086	0.3	12	17.33	1782	1730	
4	.00100	0.3	14	17.33	1740	1804	
Average	.000995	0.3	13.75	17.33	1666.5	1804	+8.2%

average computed $\lambda(.0033)$ is in good agreement (10% deviation) with $\lambda=.003$ which was used for generating the tessellations.

Delaunay model: The triangular tessellation has KV the same as in the occupancy case but with the roles of K and V interchanged-- namely, the number of neighbors of each cell is K=3 and the number of cells meeting at each vertex is V=6. Here the T.E.P. is computed using the same principle as in the occupancy case:

$$\text{T.E.P.} = p \cdot 2 \cdot \lambda \cdot S \cdot 3(1-p) \cdot \frac{32\sqrt{\lambda}}{3\pi} \cdot \frac{1}{3} = 2(1-p) \cdot pS \cdot \frac{32\sqrt{\lambda}}{3\pi}$$

$\frac{32\sqrt{\lambda}}{3\pi}$ is the expected perimeter of a triangular cell and there are three edges per cell on the average [5]. λ in the formula above is the intensity of the dual occupancy case so λ_D derived now, with data from Table 2 in [2], has to be divided by 2 to be used for computing T.E.P $(\lambda_0 = \frac{\lambda_D}{2})$. The results are given in Table 2. See Figures 3(a)-3(d) for the tessellations and 4(a)-4(d) for the corresponding colored mosaics.
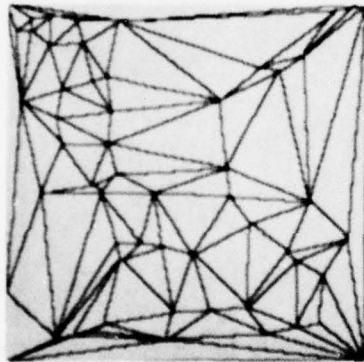
S was 200x200 and $\lambda_0=.0012$ was used to generate the tessellation. The computed λ is within 17% of the observed one; this is a consequence of the small number of measurements with high variance used to derive Table 2 in [2].
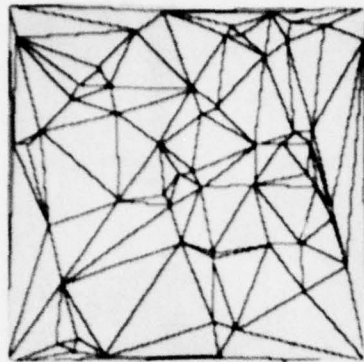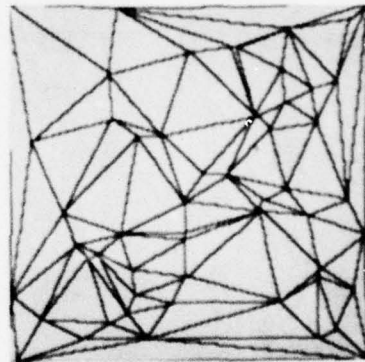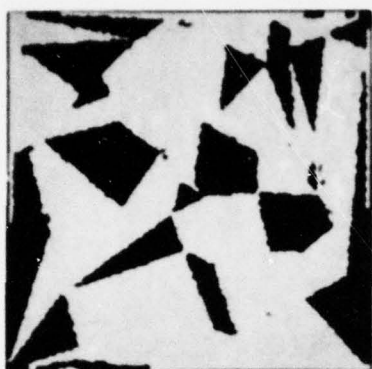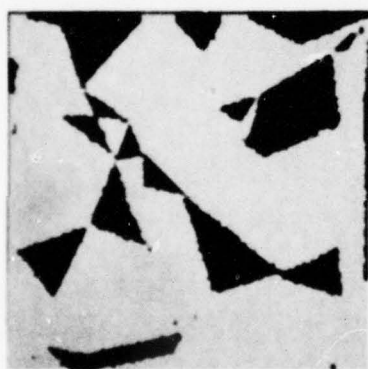
(a)
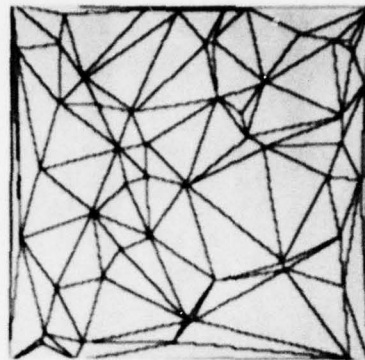
(b)

(c)

(d)

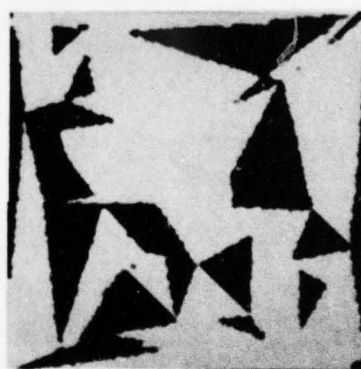Figure 3: Delaunay tessellations ($\lambda_0 = .0012$).

Figure 4: Figures 3(a)-3(d) colored with p=.3.

2.2 Natural images

We now deal with attempts to fit mosaic models to real two-color images. First the images are thresholded so as to have a definite border between object and background. Then p, the probability of object points, is estimated by the fraction of object points in the image. The number of connected components (O.N.C.C) is counted and perimeter is measured. Obviously all of the last three parameters are functions of the threshold and it should be selected so that these para eters are not sensitive to small changes in the threshold. Measurements were conducted on the interior 200x200 portion of a 510x480 picture of marble (Brodatz, D62) which is relatively sharp and easy to threshold; see Figures 5(a)-5(d). The results were: p=0.408, O.N.C.C.=27, observed perimeter=1937. Computations were done to test three image mosaic models: Poisson line, occupancy, and Delaunay. The results are as follows:

Poisson: Here $\lambda = \dfrac{T^2}{\pi}$ [5]. Thus by the considerations in Section 2.1 for computing   we derive:

$$T = \sqrt{\frac{O.N.C.C.\cdot \pi}{S\cdot \dfrac{P.N.C.C.}{10^4}}}$$

T.E.P.$=4(1-p)\cdot p\cdot (\dfrac{T^2}{\pi})\cdot S\cdot \dfrac{2\pi}{T}\cdot \dfrac{1}{4}=2(1-p)\cdot p\cdot S\cdot T$ where $\dfrac{2\pi}{T}$ is the expected perimeter of a cell. The expected number of sides of a cell is 4 [5].
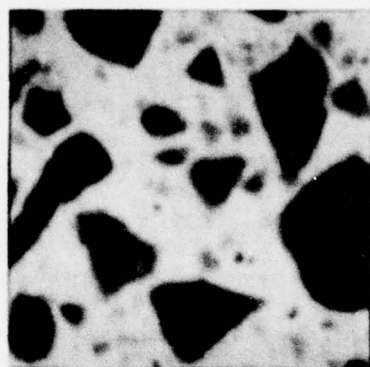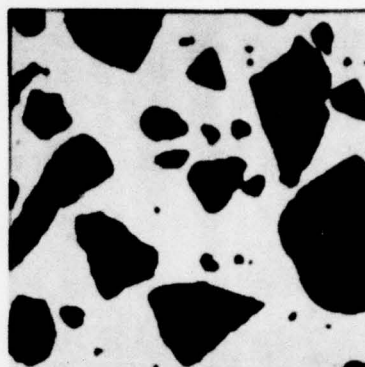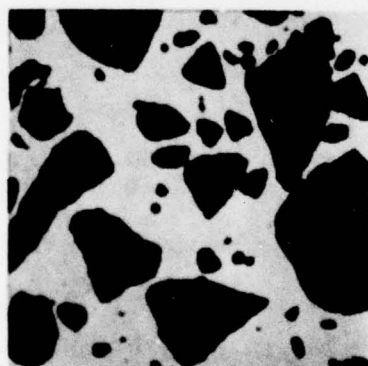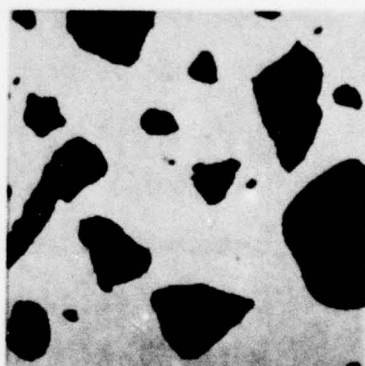
Figure 5:   (a) Brodatz's #62 marble picture

(b)-(d):   After thresholding at 25, 17,
and 36, respectively

Occupancy and Delaunay: The corresponding formulae from Section
2.1 were used.

The results for three different thresholds for the Poisson
line, occupancy and Delaunay models are presented in Tables 3-5
respectively. The Poisson line model is clearly much better
than the occupancy and Delaunay models, as might be guessed by
looking at the picture. The Poisson line results are also less
sensitive to variation of the threshold.

Table 3: Poisson line model

Threshold	O.N.C.C.	p	λ	Observed perimeter	Computed perimeter	Deviation
25	27	.408	.0062	2013	2695	+33.8%
17	36	.494	.0083	2520	3243	+29.7%
36	19	.299	.0044	1453	1975	+35.9%

Table 4: Occupancy model

25	27	.408	.0125	2013	8250	309%
17	36	.494	.0489	2520	8842	250%
36	19	.299	.00549	1453	2485	71%

Table 5: Delaunay model

25	27	.408	.00412	2013	8055	300%
17	36	.494	.0066	2520	5522	119%
36	19	.299	.00285	1453	3045	109%

3. Expected edge value

In this section we discuss the possibility of applying the analysis of Section 2 to predicting the distribution of edge values (e.g., gradient magnitudes) for an image. It is concluded that such predictions would not be very accurate.

We can view an image as composed of three basic parts: object, background and border points. If we consider the border to be sharp (this assumption will be discussed later), we measure the perimeter and compute the fraction of border points per unit area as $q = \frac{perimeter}{S}$.

Let Δ stand for the edge operator; then the expected value of Δ for the image is given by

$$E(\Delta) = E_B(\Delta)(1-p) + E_O(\Delta)(p-q) + qE_{BO}(\Delta)$$

where $E_B(\Delta)$ = expected background edge value

$E_O(\Delta)$ = expected object edge value

$E_{BO}(\Delta)$ = expected border edge value.

The term $(p-q)$ is used to correct for considering border points to be part of the object.

If we use a one-dimensional edge detector in the horizontal direction, for simplicity, then $q = \frac{perimeter}{2S}$ since on the average only half of the border segments are vertical.

Consider now a statistical model in which the object and background regions, in a picture P, are generated by independent random processes. The border is a result of interaction between them.

In fact we will compute the probability distribution of edge values in each region of P: Given two P regions, one with probability distribution $p_1(f_1)$ and the other with $p_2(f_2)$, we will compute the p.d.f. of $|f_2-f_1|$ (edge value in P), where f_1 and f_2 are grey level values in regions 1 and 2 respectively.

Now $p(|f_1-f_2|=d) = \sum\limits_{0 \le f' \le \infty} p_1(f')[p_2(f'+d)+p_2(f'-d)]$.
Assuming the p.d.f.'s are continuous and setting $x=f'$, we get
$p(|f_1-f_2|=d) = \int\limits_{-\infty}^{\infty} p_1(x)[p_2(x+d)+p_2(x-d)]dx$.

If p_1 and p_2 are $N_1(\mu_1,\sigma_1)$ and $N_2(\mu_2,\sigma_2)$ respectively, we get:

$$p(|f_1-f_2|=d) = KC_1[e^{-\alpha d^2-\beta d\cdot\gamma}+e^{-\alpha d^2+\beta d-\gamma}]$$

where

$$C_1 = \frac{1}{\sqrt{\pi(\sigma_1^2+\sigma_2^2)}} \qquad \alpha = \frac{1}{2(\sigma_1^2+\sigma_2^2)} \qquad \beta = \frac{\mu_1-\mu_2}{(\sigma_1^2+\sigma_2^2)}$$

$$\gamma = \frac{(\mu_1-\mu_2)^2}{2(\sigma_1^2+\sigma_1^2)} \qquad B = \frac{\beta}{2\sqrt{\alpha}} = \frac{\mu_1-\mu_2}{\sqrt{2(\sigma_1^2+\sigma_2^2)}}$$

$$K = \sqrt{\frac{\pi}{2}} \; \frac{1}{2-N(B)-N(-B)} \approx \sqrt{\frac{\pi}{2}}$$

$$N(B) = F_{N(0,1)}(x \le B)$$

K is the normalization factor of $p(|f_1-f_2|=d)$

Computing the expected value of $P(|f_1-f_2|=d)$ over the entire gray level range $[0,\infty]$ we get:

$$E(\Delta) = 2K[\sqrt{\frac{\sigma_1^2+\sigma_2^2}{\pi}} + (\mu_1-\mu_2)(N(B)-N(-B))]$$

where $\Delta = |f_1-f_2|$

If $\mu_1 > \mu_2$ we have B>O so that $N(B) > N(-B)$;
while if $\mu_1 < \mu_2$ we have B<O so that $N(B) < N(-B)$.

Therefore the second term in $E(\Delta)$ is always positive and thus so is $E(\Delta)$.

Assuming that the gray levels at points at distance at least 2 apart in the discrete P are independently distributed according to $N_1(\mu_1, \sigma_1)$ or $N_2(\mu_2, \sigma_2)$, $E(\Delta)$ is also true inside these regions provided we set $\mu_1 = \mu_2$ and $\sigma_1 = \sigma_2$. In this case we get $E^i(\Delta) = 2\sigma_i$ for i=1,2. In case $\sigma_1 = \sigma_2 = 0$, the formula for $E(\Delta)$ is not valid and $E(\Delta) = q \cdot (\mu_1 - \mu_2)$.

Unfortunately this model for average edge value estimation is not accurate since q, which depends on the perimeter, is not accurate. The reason is that perimeter measurement is very sensitive to the threshold applied to a picture, and yet there is no precise way to determine the correct threshold. Moreover, counting the number of connected components in the case of natural images is not accurate since we don't know beforehand which is the underlying tessellation (as we did in the case of synthetic images) and therefore which small components to discard due to thresholding errors. We also don't know which separate components close to the picture border must be considered as one because they are joined beyond the image border. The assumption of independence of gray levels at adjacent points of the picture, or even at distance 2 apart, is not always correct; this was checked in the case of the marble picture (Brodatz #62). When blur is

present, perimeter is not as well defined as in sharp images, so q is not accurate.

In summary, computing expected edge value, assuming generation of the image by a random mosaic process, cannot be expected to yield accurate results.

4. Expected width

The expected widths (run lengths) of connected components in synthetic images is analyzed in [6]. Experiments were done to test the validity of the following formulas for two-color mosaics:

Poisson line: $\quad E(\ell) = \dfrac{\pi}{2T(1-p)}$ $\qquad\qquad$ where $T = \sqrt{\lambda \cdot \pi}$

$\qquad\qquad\qquad \ell$ = run length in a component

$\qquad\qquad\qquad$ p and λ are defined in Section 2.

Occupancy: $\qquad E(\ell) = \dfrac{\pi}{4\sqrt{\lambda}\,(1-p)}$

Delaunay: $\qquad E(\ell) = \dfrac{3\pi^2}{64\sqrt{\lambda}\,(1-p)}$

Note that these formulas are singular for p=1 while the experimental width approaches the image frame width for p values near 1. Therefore the validity of the above formulas should be tested for low p values. In fact p=0.3 was used in the following experiments.

The results for four occupancy and Delaunay models are given in Tables 6 and 7. For the marble picture (Brodatz's #62) the results in Table 8 show insensitivity to threshold variations: 2.2% between the various models. As in Section 2, we use for the calculations an internal frame of a tessellation which contains cells wholly included in the original frame. Components touching the border in the internal frame are considered for run length computation, since it is believed that, on the average, the

Table 6: Synthetic Occupancy

Mosaic number	λ	p	Observed width	Computed width	Deviation
1	.003	0.3	21.402	19.47	
2	.003	0.3	20.181	19.47	
3	.003	0.3	19.066	19.47	
4	.003	0.3	19.359	19.47	
Average	.003	0.3	20.002	19.47	2.65%

Table 7: Synthetic Delaunay

Mosaic number	λ_0	p	Observed width	Computed width	Deviation
1	.002	0.3	18.01	14.76	
2	.002	0.3	15.00	14.76	
3	.002	0.3	15.27	14.76	
4	.002	0.3	16.97	14.76	
Average	.002	0.3	16.31	14.76	10.5%

Table 8: Marble picture (Brodatz #62)

Threshold	p	Observed width	Poisson	Deviation	Computed width			
					Occupancy	Deviation	Delaunay	Deviation
25	.408	20.948	19.07	8.9%	11.86	43.3%	12.19	42%
17	.494	21.062	19.27	8.5%	7.02	65.8%	11.27	46.4%
36	.299	21.427	19.14	10.6%	15.11	29.4%	12.43	42%

The appropriate λ for each mosaic model appears in Tables 3-5.

correct width of a border-touching component is encountered inside the image.

As in the case of perimeter, the Poisson line process best predicts the observed run length of a component in the marble picture (#62). In fact it is four **times** better than the predictions of the other two mosaic models. Moreover, in the width case the deviation between the observed and predicted value is at most 10% (Poisson model), which is much less than the deviation in the perimeter case for the Poisson model (34%).

5. Conclusions

a) Results for expected perimeter in two-color synthetic tessellations are in very good agreement with observations.

b) Results for real images are not very good. Some models fit an order of magnitude better than others, but reliable conclusions can be drawn only after trying more real images. Using perimeter evaluation for estimating the edge value density of real images will not be accurate, due to its dependence on the thresholding process which is not accurately defined.

c) For real images, where thresholds are used to distinguish between objects and background, the width is much less sensitive than the perimeter to variations in the threshold, and therefore is a much better measure for determining the generating tessellation.

References

[1] Ahuja, N., "Connectivity in lattices and mosaics," TR-637, Computer Science Center, Univ. of Maryland, February 1978.

[2] Ahuja, N., "Connectivity in lattices and mosaics II," TR-677, Computer Science Center, Univ. of Maryland, June 1978.

[3] Ahuja, N., "Geometrical properties of bombing patterns," TR-673, Computer Science Center, Univ. of Maryland, June 1978.

[4] Ahuja, N., "Connectedness properties of bombing patterns," TR-682, Computer Science Center, Univ. of Maryland, July 1978.

[5] Schachter, B. J., Rosenfeld, A., and Davis, L. S., "Random mosaic models for textures," TR-463, Computer Science Center, Univ. of Maryland, July 1976; IEEE Tran. Systems, Man, Cybernetics SMC-8, 1978, 694-702.

[6] Ahuja, N., "Mosaic models for image analysis and synthesis," Ch. 4, doctoral dissertation, University of Maryland, March 1979.

REPORT DOCUMENTATION PAGE		READ INSTRUCTIONS BEFORE COMPLETING FORM
1. REPORT NUMBER	2. GOVT ACCESSION NO.	3. RECIPIENT'S CATALOG NUMBER
4. TITLE (and Subtitle) PREDICTED PROPERTIES OF MOSAIC IMAGES		5. TYPE OF REPORT & PERIOD COVERED Technical
		6. PERFORMING ORG. REPORT NUMBER TR-746
7. AUTHOR(s) Tsvi Dubitzki, Narendra Ahuja, and Azriel Rosenfeld		8. CONTRACT OR GRANT NUMBER(s) DAAG-53-76C-0138
9. PERFORMING ORGANIZATION NAME AND ADDRESS Computer Science Center University of Maryland College Park, MD 20742		10. PROGRAM ELEMENT, PROJECT, TASK AREA & WORK UNIT NUMBERS
11. CONTROLLING OFFICE NAME AND ADDRESS U. S. Army Night Vision Laboratory Ft. Belvoir, VA 22060		12. REPORT DATE March 1979
		13. NUMBER OF PAGES 25
14. MONITORING AGENCY NAME & ADDRESS(if different from Controlling Office)		15. SECURITY CLASS. (of this report) Unclassified
		15a. DECLASSIFICATION/DOWNGRADING SCHEDULE

16. DISTRIBUTION STATEMENT (of this Report)

Approved for public release; distribution unlimited.

17. DISTRIBUTION STATEMENT (of the abstract entered in Block 20, if different from Report)

18. SUPPLEMENTARY NOTES

19. KEY WORDS (Continue on reverse side if necessary and identify by block number)

Image processing
Pattern recognition
Texture analysis
Image modeling

20. ABSTRACT (Continue on reverse side if necessary and identify by block number)

This paper considers the computation of the expected perimeter of a component in mosaic image models and checks its applicability to real images. The expected width of a component in the Occupancy and Delaunay models and in a real image is also considered.